Accuracy and sensitivity of radium mass balances in assessing karstic submarine groundwater discharge in the stratified Calanque of Port-Miou (Mediterranean Sea)

Christelle Claude, Sabine Cockenpot, Bruno Arfib, Samuel Meulé, Olivier Radakovitch

Journal of Hydrology
Volume 578, November 2019, 124034

Research papers

Accuracy and sensitivity of radium mass balances in assessing karstic submarine groundwater discharge in the stratified Calanque of Port-Miou (Mediterranean Sea)

Christelle Claude [a], Sabine Cockenpot [a], Bruno Arfib [a], Samuel Meulé [a], Olivier Radakovitch [a, 1]

https://doi.org/10.1016/j.jhydrol.2019.124034

Accuracy and sensitivity of radium mass balances in assessing karstic submarine groundwater discharge in the stratified Calanque of Port-Miou (Mediterranean Sea).

Christelle Claude[1], Sabine Cockenpot[1], Bruno Arfib[1], Samuel Meulé[1], Olivier Radakovitch[1, 2]

1. Aix Marseille Univ, CNRS, IRD, INRA, Coll France, CEREGE, Aix-en-Provence, France
2. Presently at: Institut de Radioprotection et de Sureté Nucléaire (IRSN), PSE-ENV/SRTE/LRTA, BP3, 13115 Saint-Paul-Lez- Durance, France.

Abstract

Submarine Groundwater Discharge (SGD) has received increased attention in recent years since it was recognized that it may be both volumetrically and chemically important. Around the Mediterranean Sea, 60% of the coastline is composed of karstic aquifers, and to properly estimate the hydrological budget of the Mediterranean Sea it is therefore necessary to better assess the karstic submarine groundwater discharges (KSGD). However, quantifying KSGD is still challenging. Among the methods recently developed to detect and quantify SGD, the mass balance method of the radium quartet ^{223}Ra, ^{224}Ra, ^{226}Ra and ^{228}Ra has proved to be a powerful technique. This approach requires characterizing all the contributing terms and sinks in the coastal water volume affected by SGD, the residence time of coastal waters, as well as a representative concentration of the tracers for both surface water and discharging groundwater. In this study we combine several approaches (^{223}Ra, ^{224}Ra, salinity profiles and Acoustic Doppler Current Profiler (ADCP) measurements) to examine both the accuracy and sensitivity of the radium mass balance method in the case of the cove of Port-Miou (Mediterranean Sea, France) where the main karstic spring discharges locally at 10 m depth. This study benefits from the inland in-situ access to the main karst conduit discharging to the sea which provides a long time series to characterize

the brackish submarine groundwater end-member. We show that the composition of the cove water is stratified, with two water bodies: a surface brackish layer and a deeper layer. The mean KSGD value obtained with ^{223}Ra and ^{224}Ra mass balances in the surface water body is precise but significantly lower (0.6 ± 0.1 m^3/s) than the karstic spring discharge (4 ± 1 m^3/s) estimated within the karst conduit with pressure sensors. The residence time of the cove water estimated using both ^{224}Ra and ^{223}Ra isotopes is very low (1 ± 1 day). Our study shows that the water residence time that we calculated using the Ra mass balance is the key parameter that may impact KSGD. In addition, based on ADCP transects, we suggest that the shape and geometry of the cove, as well as the location of the discharge point of the spring play a key role in explaining these discrepant results. We therefore recommend that in such stratified coves, estimations of KSGD based on short-lived radium isotopes require accurate and independent estimates of the water residence time as well as a good knowledge of the shallow and deep circulation patterns of the cove water.

Key words

Coastal karstic aquifer, Mediterranean Sea, Submarine groundwater discharge, radium isotopes

Highlights:

- Kartic groundwater discharge (KSGD) in a major European karst spring estimated
- Radium tracer methods compared with salt, water mass balances and direct flow measurements
- KSGD with radium tracers precise but significantly lower than direct flow measurements
- Knowledge of both water residence time and shallow and deep circulation patterns needed

1. Introduction

Submarine Groundwater Discharge (SGD) has received increased attention during the last few decades since it was recognized that it may be both volumetrically and chemically important (Johannes, 1980; Moore, 1996a; Ferguson and Gleeson, 2012; Moosdorf and Oehler, 2017). Investigations into fresh groundwater inputs into the sea were initially related to water resource purposes, but there is now a growing consensus that SGD includes both fresh groundwater and re-circulated seawater, and that it may be an important pathway for material transport from land to the ocean, playing a relevant role in coastal ecology and geochemical cycles of several compounds such as nutrients, metals, carbon or pollutants (see several review articles: Burnett and Dulaiova, 2003, 2006; Charette et al., 2008; Knee and Paytan, 2011; Moore, 2010; Santos et al., 2012; Slomp and Van Cappellen, 2004; Swarzenski, 2007).

Many studies published on this subject were performed at the scale of long coastlines of tens or hundreds of kilometers where porous aquifers are discharging (e.g., Moore et al., 2008; Peterson et al., 2009; Waska & Kim, 2011; Lamontagne et al., 2015) or in large lagoons (e.g. Rapaglia et al., 2010; Baudron et al., 2015). In these cases, the submarine groundwater whatever its origin, terrestrial or marine as defined by Stieglitz et al. (2013), circulates into the sediments, mixes with the pore water and flows at the sediment-water interface.

Recently, Rodellas et al. (2015) used ^{228}Ra activities in a mass balance approach to calculate that SGD inputs along the Mediterranean shoreline. They found that they may range from 6 to 100.10^6 m^3/km/yr, which corresponds to 1.2 to 19 times the fluxes coming from the rivers (Ludwig et al., 2009), including

both fresh groundwater and re-circulated seawater. Around the Mediterranean Sea, 60% of the coastline is composed of karstic aquifers. In addition, first estimates based on hydrogeology indicated that they may contribute up to 75% of the total fresh water inputs to the Mediterranean Sea (UNESCO, 2004; Custodio 2010; Bakalowicz, 2015). To properly estimate the hydrological budget of the Mediterranean Sea it is therefore necessary to better estimate the karstic submarine groundwater discharges (KSGD).
SGD-related research has mainly focused on the development of new techniques to detect and quantify SGD, in particular radium isotopes (^{223}Ra, ^{224}Ra, ^{226}Ra, ^{228}Ra), radon (^{222}Rn) or other tracers (Moore, 1996a& b; 2003). The radium tracers are usually enriched in coastal groundwater relative to coastal seawater and behave conservatively once released to the coastal ocean. Since their half-lives range from 3.7 days to 1600 years, they can be incorporated to mass balances in order to estimate SGD flows on a variety of time-scales and they can be used to distinguish different groundwater sources and also to estimate the residence time of coastal waters (Charette et al., 2008). The mass balance approach requires defining the boundaries of the system investigated (represented as a box of coastal waters receiving the SGD), and characterizing all the terms and sinks contributing to the radionuclide concentrations within this box. It includes the volume of the coastal water study site, the water residence time as well as a representative concentration of the tracer for both surface water and discharging groundwater. It relies on the hypothesis that their concentrations are uniform in the water column, and samples collected just below the surface are taken as representative of the whole system, whatever the water depth. Thus, the water column is assumed to present a homogeneous and integrated signal of the natural tracers entering the system via groundwater pathways.
In the case of karstic aquifers, carbonate rocks contain karst conduits that play the role of preferential pathways connecting the fissured rock (matrix flow) and the karst network (e.g. Ford and Williams, 2007). Flows are thus highly heterogeneous and groundwater discharges usually occur at very specific points corresponding to springs, leading to high discharge rates in a few outlets draining the whole recharge area. Furthermore, these springs may be located below or just at the surface of the sea level (Fleury et al., 2007) and the associated brackish or freshwater plume may induce a stratification in the water column (Garcia-Solsona et al., 2010a & b). Montiel et al. (2018) showed that methods to assess SGD should be adapted in the case of karstic submarine springs, and they highlighted that there are still many field difficulties that can corrupt the correct estimation of the SGD.
The aim of this paper was to test the reliability and accuracy of the ^{223}Ra-^{224}Ra tracer technique to estimate SGD in a coastal karstic environment where the SGD concentrates in point sources of discharge, i.e. at submarine springs, and then mixes and spreads in the sea-water column, yielding 3D salinity, temperature or tracer concentration contrasts. Therefore, the estimate requires adapting the field data survey and the calculation model. This study focuses on the Port-Miou brackish submarine spring (SE France) discharging into a natural cove (called calanque). This case study offers two main advantages: i) the shape of the calanque limits the exchanges (inflow and outflow) with the open sea at the mouth of the natural cove ii) the discharge and salinity of the submarine spring are monitored by continuous in-situ sensors at a gauging station in the flooded karst conduit located 500 meters upstream of the sea (underground laboratory). Moreover, this spring is one of the major sources of SGD to the Mediterranean Sea in Europe (Tulipano et al. 2005; Custodio 2010; Arfib and Charlier, 2016). In addition, there is no sediment or runoff, which means that a simplified radium mass balance can be performed.

2. Site description: the calanque and the karstic coastal aquifer of Port-Miou

The calanque of Port-Miou is located in the bay of Cassis, 15km from Marseille city (SE France). It is a kind of cove, a small dry valley cut into the tight early Cretaceous limestone (Urgonian facies) from

the land to the sea (Fig. 1). The term "calanque" will be used in the remainder of this paper to refer to the submerged part of the valley, where the sea enters between steep rocky cliffs. The calanque is oriented NE-SW. It is 1.3 km long but is very narrow (20 m wide, on average) and its shape is very similar to other calanques between Marseille and Cassis. The water depth increases slowly from 0 at the NE down to 25 m at the outlet of the calanque, where it is directly connected to the sea. The flux of water exchanged between the calanque and the coastal sea is unknown, but it may be driven by the groundwater discharge and the wind.

Port-Miou is one of the largest karst springs in Europe, with an average annual brackish discharge ranging between 3 and 8 $m^3.s^{-1}$ (Tulipano et al., 2005; Custodio, 2010; Bakalowicz, 2015; Arfib and Charlier, 2016; Chen et al., 2017). The catchment area extends mainly over a natural landscape made of hills, karst plateau, and polje. The northern boundary of the recharge area is not well-known, but considering the geological context, the area was evaluated at 400 km^2. Several springs discharge into the calanque of Port-Miou. The main spring discharge occurs around 10m water deep on the southern western flank of the calanque, and corresponds to a large karst conduit open to the sea. It has been explored from the outlet by cave-divers who discovered a huge saturated sub-horizontal 20m diameter karst conduit developing more than 2 km inland (Arfib & Charlier 2016). Other small springs occur at sea level on the northern side of the calanque (Fig. 1 and appendix A2).

In the 70s, a submarine dam was built in the main karst conduit, 500 m inland, with a man-made access via an underground tunnel and shaft. Groundwater flows through pipes across the dam that blocks the karst. The dam was built with the aim of decreasing the groundwater salinity. It stopped the direct intrusion of shallow water upflowing from the sea by the mouth of the spring, but the groundwater remained brackish, showing that the seawater intrusion encroaches the aquifer in depth, upstream the spring and the dam. Regular in-situ measurements at the dam and at the northern springs in the calanque showed that groundwater salinity and temperature are similar. These outlets discharge the same aquifer throughout the year and give access to the groundwater. Since the 2000s, this dam has been equipped with pressure sensors to monitor the groundwater discharge and the salinity (Fig. 2). The recent study by Arfib and Charlier (2016) based on 4 years of data from 2011 to 2014 (rainfall, discharge and salinity time-series) proposed a conceptual model of saline intrusion suggesting that the salinity results from seawater intrusion by the mixing of a deep brackish groundwater reservoir with shallow fresh groundwater.

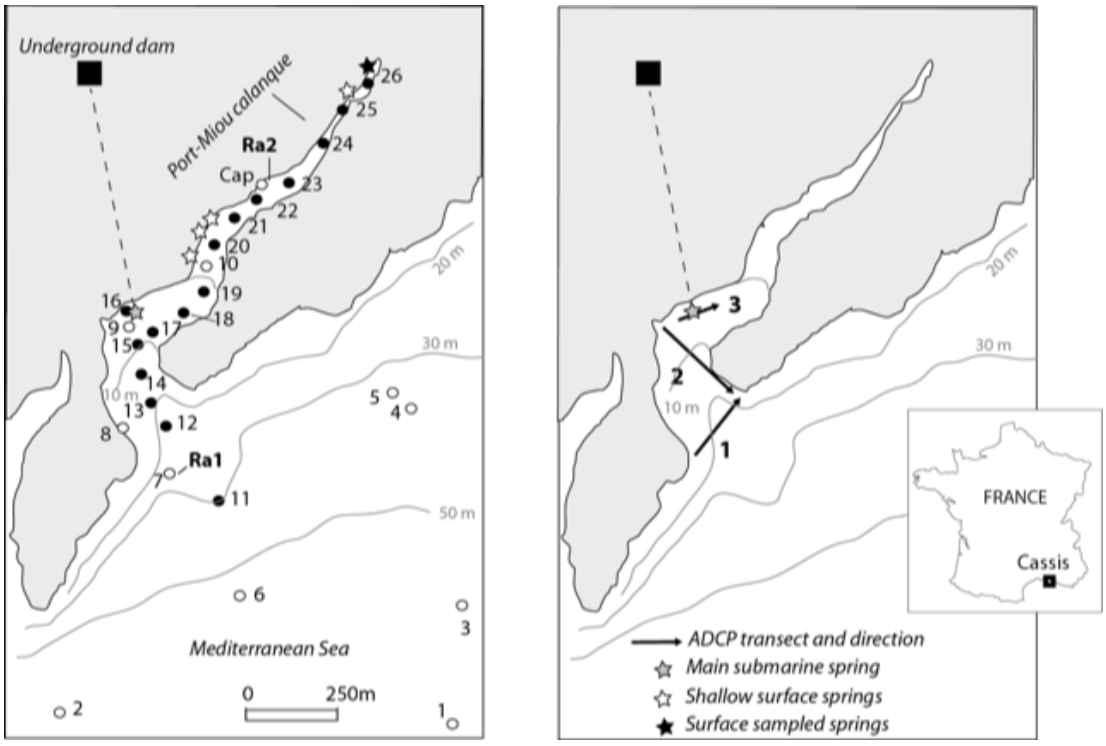

Figure 1: Location map and numbers (#) of samples (hereafter labelled PM#) collected in the Calanque of Port-Miou in 2012 and 2014. Ra1 and Ra2 are the radium depth profiles measured at the location of sample #7 and #Cap, respectively. ADCP Transects 1, 2 and 3 are also reported. The black square is the location of the dam.

3. Data

3.1 Sampling

As pointed out by Montiel et al. (2018), the selection of a representative groundwater end-member is a critical component of any tracer study. Groundwater samples were collected upstream the underground dam in the karst conduit (hereafter called "dam groundwater samples") and at the northern outlets (hereafter called "spring groundwater samples") systematically the day before collecting the calanque and coastal waters. Two field campaigns were performed, in July 2012 and September 2014. Additional samples were also collected in January and March 2013 in order to explore the variability of radium composition with time (Table 1, Fig. 1). These sampling locations give access to the brackish groundwater discharging to the sea, without shallow seawater intrusion pollution at the dam, and with a very low pollution at the northern springs. Continuous in-situ salinity measurements at the Port-Miou underground dam, which are essential for the salt mass balance, are scarce but would enable the uncertainty of the SGD estimate to be reduced (Cerdà-Doménech et al., 2017).

Calanque and coastal water samples were also collected during the two field campaigns. In July 2012, most of the samples were taken from the coastal water in front of the exit of the calanque, while in September 2014 they were taken mainly in the calanque itself (Fig. 1). Temperature and salinity were measured with an HQ40d multiparameter probe (Hach).

In addition, vertical profiles of salinity and temperature of the water column were obtained during the September 2014 campaign, at each sampling location in 2014 with a CTD-DIVER datalogger (Fig. 3). Salinity (PSU) was calculated from specific conductivity measurements using the sheet available from Aminot and Kerouel (2004).

3.2 Radium measurements

Samples were collected in surface water (about 0.5 m deep) by pumping water into a plastic container for the analysis of radium. Some vertical profiles of ^{223}Ra and ^{224}Ra were also sampled in July 2012, January 2013 and August 2014 using a Niskin bottle (Fig. 1). The volume of water samples ranged from 15 (groundwater) to 60L (coastal waters). Radium isotopes were extracted by passing water samples by gravity through a PVC cartridge filled with 20 g dry weight of manganese oxide-impregnated acrylic fiber ("Mn-fiber"). The water flow rate was kept at less than 1 L per minute in order to ensure that the retention capacity of the Mn-fiber was higher than 97% (Moore, 2008). Before processing the sample, the water content of each Mn-fiber was kept between 0.4 and 1.1 gH2O/gfiber in order to obtain maximum emanation efficiency (Sun and Torgersen, 1998). The samples were processed with the RaDeCC system for ^{223}Ra and ^{224}Ra (Radium Delayed Coincidence Counting).

^{223}Ra and ^{224}Ra activity measurements with RaDeCC were calibrated using 4 in-house mono-isotope standards of ^{227}Ac and ^{232}Th (the parent isotopes of ^{223}Ra and ^{224}Ra respectively) and 4 multi-isotope standards, containing ^{227}Ac, ^{232}Th and ^{226}Ra. All standards were prepared according to the technique of Scholten et al. (2010). The detection efficiencies of our four detectors were very similar and close to the values reported in Scholten et al. (2010). Changes with time occurred within the error range. All errors were calculated according to Garcia-Solsona et al. (2008b).

The activity of ^{228}Th in water was processed with RaDeCC one month after collection measuring supported ^{224}Ra activity in equilibrium with ^{228}Th. ^{227}Ac activity in water was processed with RaDeCC 3 months after collection measuring supported ^{223}Ra in equilibrium with ^{227}Ac. Further details of the analytical technique are reported in Baudron et al. (2015) and Cockenpot (2016).

3.3 Karst spring discharge and salinity

Direct measurement of the groundwater discharge is available inland, in the karst conduit 500 meters upstream the main Port-Miou submarine spring. The discharge is estimated by the head losses generated by the flow through the gates of the underground and submarine dam built across the karst conduit in the 1970s. Head measurements upstream ($H_{Upstream}$) and downstream ($H_{Downstream}$) the dam with pressure sensors were converted into discharge by the general Bernoulli hydraulic equation for submerged flow:

$$Q = K.\sqrt{\Delta H} \quad (1)$$

with Q the karst groundwater discharge, K a coefficient that accounts for losses, area and units conversion, and $\Delta H = H_{Upstream} - H_{Downstream}$. ΔH was calibrated with direct measurements of H using a level surveyor a few days before the sampling. K had been calibrated by direct discharge measurement using the dilution method of fluorescent dye (Schnegg et al. 2011) injected upstream in the karst conduit by cave-divers. Head measurements used Cera-Diver sensors, with 0.5 cm H_2O typical accuracy. Propagating the error using the variance formula yielded between 10% and 25% of uncertainties at discharge states of 3 to 4 m^3/s. The daily average value was calculated using the 20-second sampling interval measurements.

A previous study by Arfib and Charlier (2016) based on 962 days of salinity and discharge data (daily average, non-continuous data from Dec. 16th 2010 to Dec. 11th 2014) showed that discharge can be roughly estimated by salinity measurements or by applying a lumped rainfall-salinity-discharge model. In-situ salinity was monitored with a CTD-Diver sensor at a 15-minute time step.

3.4 Current measurements

Three transects of vertical profile of flow velocity were collected in the calanque in September 2014. The objective was to evaluate the flow structure between the calanque and the open sea. The data set

was acquired using a downward looking ADCP Workhorse Sentinel 600 kHz (Teledyne RDI) mounted on a powered boat. The bin size was set to 50 cm.
Due to the blanking distance and the transducer depth, the first cell of measurements was approximately around 1m below the surface layer. The size of the near-bed blank zone depends on water column depth, but for water depths of 20 m, the blank may be estimated around 1.2 m. Due to this problem of blank inherent to the ADCP system, it was not possible to obtain the current velocities or directions within the brackish surface layer and above the bottom. Consequently, the flow rate exchange between the calanque and the sea was not estimated with ADCP measurements. The locations of the 3 transects are pinpointed on Fig 1. Transect 1 is located at the entrance of the calanque. Transect 2 is located in the middle of the calanque. Transect 3 was set to pass just above the submarine spring (not visible from the surface). The data were continuously geo-referenced by a vessel-mounted Trimble DGPS. The raw data were averaged at each depth over 10 ensembles. The data cell length is about 7 to 10m in the horizontal direction.

4 Method:

4.1 The radium mass balance approach to estimate SGD

The mass balance approach also called "radium box model" was developed by Moore (1996a) and has been applied in numerous studies worldwide (Charette et al., 2001; Kim et al., 2003; Beck et al., 2007; Garcia-Solsona et al., 2008a; Moore et al., 2008; Ollivier et al., 2008; Baudron et al., 2015, Rodellas et al., 2015;). By constraining all the potential Ra sources and sinks within a box studied (defined as the volume of coastal water affected by SGD), the Ra flux supplied by SGD can be estimated by the difference between inputs and outputs assuming steady state (equation 1). In our case, this steady–state mass balance can be significantly simplified, because there is no surface water flow into the calanque and only a very thin layer of sediment over the bedrock (thus no diffusion from porewater).

$$Ra_{SGD} + Ra_{in} + Ra_{prod} = Ra_{out} + Ra_{dec} \quad (2)$$

All Ra fluxes are in Bq.d^{-1} and all Ra activities are in Bq.m^{-3}.

Ra inputs include SGD (Ra_{SGD}) and in situ radioactive production from the parent isotope (Ra_{prod},).

$$Ra_{prod} = (\lambda . ARa' . V) \quad (3)$$

ARa' is the Ra activity of the parent of the Ra isotope considered. λ (d^{-1}) is the decay constant of the isotope considered. V (m^3) is the water volume of the calanque affected by SGD.

Ra is lost from the system by radioactive decay (Ra_{dec}) and by export offshore (Ra_{off}).

$$Ra_{dec} = (\lambda . ARa . V) \quad (4)$$

ARa is the average activity of the water column in the study site.

$$Ra_{Off} = Ra_{out} - Ra_{in} \quad (5)$$

Ra_{off} is the difference between the input of radium from the coastal waters into the calanque (Ra_{in}) and the export of radium from the calanque to the coastal waters (Ra_{out}). Raoff can be calculated as follows:

$$Ra_{Off} = \frac{(ARa - ARa_{in}) * V}{T_w} \quad (6)$$

ARa_{in} is the Ra activity in the coastal water.
T_w (d) the apparent age of coastal waters.

The submarine water discharge Q_{SGD} can be calculated by resolving equation (7), dividing by the radium activity of the groundwater end-member (ARa_{SGD}) (equation (8)).

$Ra_{SGD} = Ra_{out}$ - Ra_{in} + Ra_{dec} - Ra_{prod} (7)

$$Q_{SGD} = \frac{Ra_{SGD}}{ARa_{SGD}} \quad (8)$$

To solve equation (7) and calculate Ra_{SGD}, there is only one unknown, T_W.

Pairs of Ra isotopes can be used to estimate the water apparent age, defined as the time a water parcel has spent since entering the study site through one of its boundaries (Moore, 2000; Monsen et al., 2002; Moore et al., 2006). Ra-based approaches to estimate water ages are based on the variation of Ra activity ratios due to the time elapsed since Ra isotopes became disconnected from their source (i.e. SGD). Moore et al. (2006) has described the case where Ra inputs occur with multiple springs:

$$T_w = \frac{AR_{SGD} - AR_{in}}{AR_{in} . \lambda_S} \quad (9)$$

$$AR = \frac{(ARa_{short} - ARa'_{short})}{(ARa_{long} - ARa'_{long})} \quad (10)$$

where AR_{in} and AR_{SGD} are the excess activity ratios (equation (9)) of the radium activities of the shorter-lived Ra isotope (^{224}Ra) to the longer-lived Ra isotope (^{223}Ra) in the coastal waters and SGD, respectively, and λ_S is the decay constant of the shorter-lived isotope. Excess activities are un-supported activities (relative to the parent isotope).

4.2 Water, salt and radium mass balance

A second mass balance approach can be achieved by combining water, salt and the radium mass balances in order to estimate the flux of coastal water entering the calanque (Q_{in}), the flux of calanque water flowing out of the calanque to the sea (Q_{out}) and the groundwater discharge to the calanque (Q_{SGD}).

Water mass balance:

All water fluxes (Q) are in $m^3.d^{-1}$.

$$Q_{SGD} + Q_{in} = Q_{out} \quad (11)$$

Salt mass balance:

$$Q_{SGD} . S_{SGD} + Q_{in} . S_{in} = Q_{out} . S_{out} \quad (12)$$

S_{SGD} is the salinity of the groundwater, S_{in} is the salinity of the coastal water and S_{out} is the average salinity of the calanque.

Radium mass balance (^{224}Ra or ^{223}Ra) combined with the water mass balance:

The Ra mass balance (in $Bq.d^{-1}$) can be written as follows:

$$Q_{SGD} . ARa_{SGD} + Q_{in} . ARa_{in} + Ra_{prod} = Q_{out} . ARa_{out} + Ra_{dec} \quad (13)$$

This system of 3 equations can be solved by:

$$Q_{out} = \frac{Ra_{dec} - Ra_{prod}}{ARa_{SGD} . \left(\frac{S_{in} - S_{out}}{S_{in} - S_{SGD}}\right) + ARa_{in} . \left(\frac{S_{out} - S_{SGD}}{S_{in} - S_{SGD}}\right) - ARa_{out}} \quad (14)$$

$$Q_{in} = \frac{Ra_{dec} - Ra_{prod}}{ARa_{SGD} \cdot \left(\frac{S_{in} - S_{out}}{S_{out} - S_{SGD}}\right) - ARa_{out} \cdot \left(\frac{S_{in} - S_{SGD}}{S_{out} - S_{SGD}}\right) + ARa_{in}} \quad (15)$$

5. Results

5.1 Karst aquifer behavior and dam groundwater discharge

Four years of discharge and salinity time series of the Port-Miou karst spring (recorded at the dam) are plotted in Figure 2. From 2010 to 2014, discharge ranged from 3 m^3/s at the end of the low-flow period to 37 m^3/s during flood. The spring is characterized by a typical karst-type functioning with high-flood events related to rainfall, and a high base-flow discharge. As usually observed in coastal karstic springs (Fleury et al., 2007), the water is brackish, due to deep saline intrusion (Arfib and Charlier, 2016). Salinity is correlated with discharge, with drop during flood events. Except during floods, salinity variations are very smooth, with a seasonal trend. The lowest salinities reached 2 g/L, whereas highest salinities increased up to 13 g/L. At the 15-minute recording time step, salinity did not vary over the day, with no influence of the sea-tide. The two radium campaigns were done during the low-flow period, in summer (July 2012, September 2014). There had been no floods over the preceding month, and no significant rainfall events. The salinity of the submarine groundwater discharge to the calanque remained constant during the field campaigns. Discharge measurements were not available during the 2012 campaign (Figure 2), but a rough estimate of around 4 m^3/s can be given using the lumped model of Arfib and Charlier (2016). In September 2014, karst discharge measurement at the underground dam was also close to 4 ± 1 m^3/s using the previously defined 25% error. Considering the salinity and discharge data as representative of the hydrological functioning of the aquifer, the 2012 and 2014 field campaigns were in a similar condition.

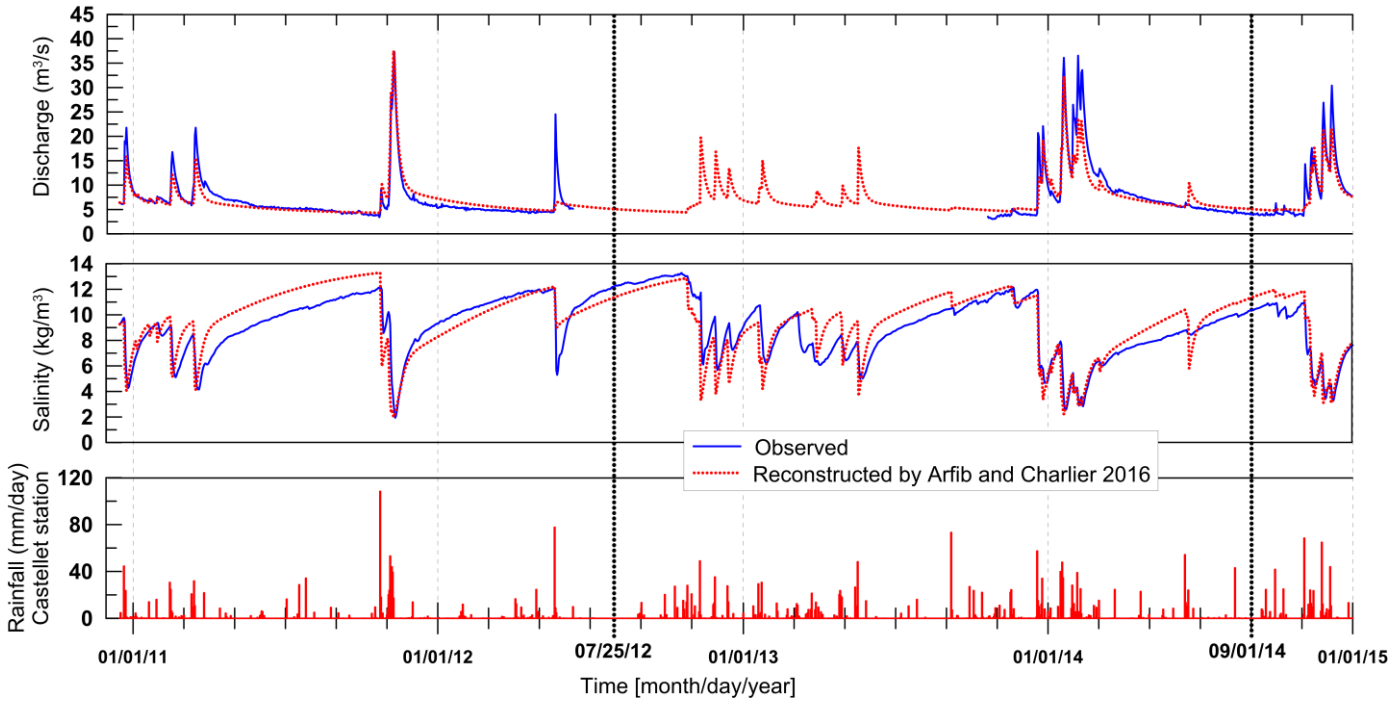

Figure 2: Salinity and discharge time series recorded (observed) at the Port-Miou brackish spring (underground dam, in the karst conduit 500 meters upstream the outlet to the sea). Simulated time series with the lumped rainfall-salinity-discharge model (Arfib and Charlier, 2016). Rainfall at the meteorological station Le Castellet, in the catchment area (Météo-France). The two vertical dotted lines refer to the time of the radium campaigns.

5.2 Salinity and temperature samples

Five samples of groundwater were collected during and in between the two campaigns (three upstream of the dam and two at the northern springs). The temperature upstream the dam and in the spring samples were not significantly different (16.8 ±0.6 °C). The salinity was on average very stable upstream the dam (9.9 ± 0.2) but slightly higher and more variable at the northern spring (11 ± 1). This range falls in the higher band of the multi-year variability measured between 2011 and 2014 (Fig. 2).

In the calanque, the salinity of the surface samples collected in 2012 and 2014 ranged between 23.7 and 36.7 (Table 2). The salinity of the coastal water outside the calanque was between 34.5 and 38.5.

Vertical profiles of temperature and salinity were done at each location where surface water was collected for radium isotopes (Fig. 3). Measurements were performed every meter from the surface down to 10 meters deep. All profiles showed the same pattern characterized by a stratified surface layer between 1 and 2 m deep where the salinity increases slowly up to one similar to the seawater, until the bottom (38, Fig. 3). Plots of temperature against salinity showed the existence of these two water masses: the water mass I, which is less saline and warmer, and the water mass II similar to the sea water (Fig. 3).

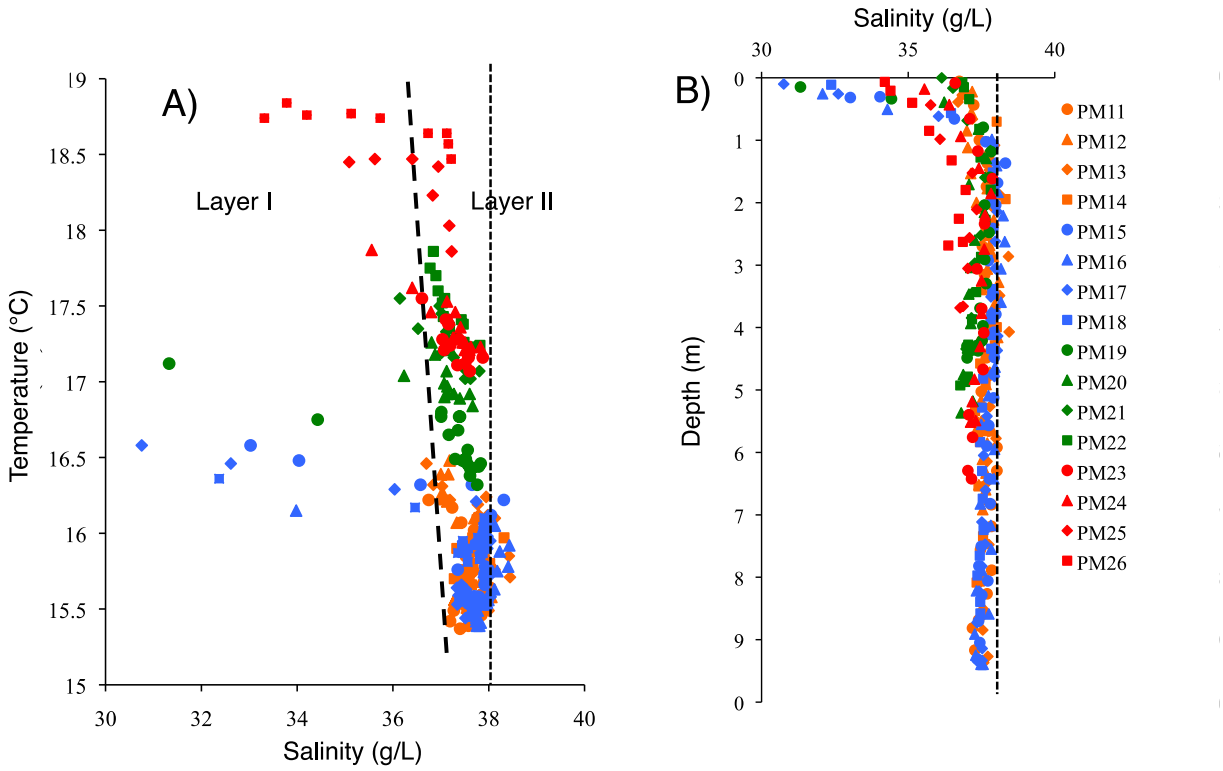

Figure 3: A) Temperature (°C) against salinity and B) Salinity against depth. Salinity in surface samples collected in 2014 in the calanque of Port-Miou showing a vertical stratification where two water masses are recognized on both sides of the dashed line (Layer I and layer II): Layer I is the surface layer impacted by the contribution of the Port Miou spring water discharge. Layer II is the underlying sea water displaying a salinity of 38 g/L (dotted line). Location of samples refers to Figure 1.

5.3 Radium isotope data

Radium isotopes are reported with salinity and temperature data in Table 2. In groundwater samples, ^{224}Ra and ^{223}Ra activities are not significantly different in samples collected upstream the dam and at the

different outlets, attesting a similar groundwater origin. The activity values were on average 23 ± 1 and 2.2 ± 0.4 Bq/m3 for ^{224}Ra and ^{223}Ra (Table 1).

The activities of ^{224}Ra and ^{223}Ra in the surface samples from the calanque ranged respectively from 4.3±0.2 to 13±1, and from 0.40±0.04 to 1.6±0.1 Bq/m3. Measurements in the coastal water return lower values, ranging between 2.50±0.08 and 0.20±0.01 for ^{224}Ra, and between 0.008±0.003 and 0.20±0.02 Bq/m3 for ^{223}Ra. ^{228}Th activities were on average 0.5 Bq/m^3 in the calanque (Table 2). ^{223}Ra and ^{224}Ra are linearly correlated and are also correlated with the salinity, plotting on a two end-member mixing line, between the groundwater and the coastal water end-members (Fig. 4). A similar relation was also found by Bejannin et al. (2017) in the same area.

Salinity and ^{224}Ra vertical profiles were measured at two stations: PM7, during the campaign of July 2012 and PM-CAP, in January 2013 and end of August 2014, a few days before the campaign. ^{224}Ra and salinity were still correlated, showing the stratified water column composed of the surface layer with lower salinity and a higher ^{224}Ra activity and a lower layer which has the same salinity and ^{224}Ra as coastal water (Fig. 5).

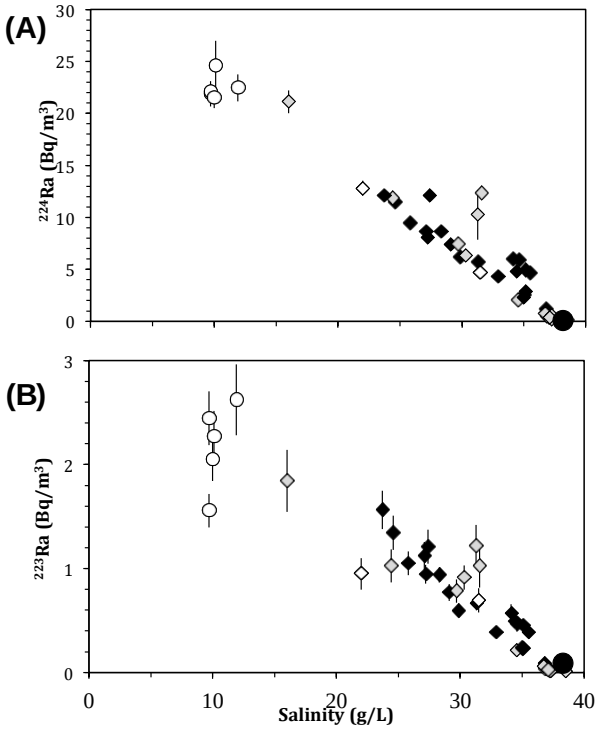

Figure 4: (A) ^{224}Ra and (B) ^{223}Ra against salinity in the Port Miou main karstic spring (open circles), the surface waters and the depth profiles Ra1 and Ra2 in the calanque of Port-Miou. Error bars are 1σ. Black diamonds are data collected in 2014, gray diamonds are data collected in 2012, open diamonds are data collected in 2013. The black circle indicates the value of coastal seawater.

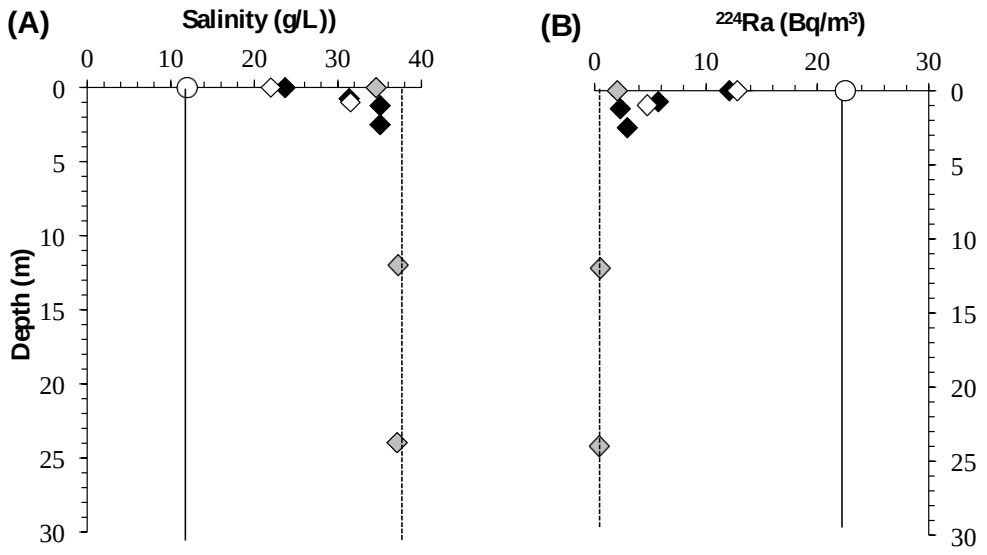

Figure 5: Salinity (A) and ^{224}Ra (B) against depth at the location of PM7 (2012) and at the location of PM_Cap in January 2013 and August 2014. The black dotted line at 38 g/L and 0.4 Bq/m3 for salinity and ^{224}Ra respectively, indicates the seawater value. The black line at 10 g/L and 22 Bq/m3 for salinity and ^{224}Ra respectively, indicates the value of the karstic spring. Error bars are smaller than the symbols. The symbols are the same as in Fig. 4.

5.4 Current measurements

The transects of current are reported on Fig. 6 and their locations are given on figure 1.

At large scale, the surface layer is clearly a wind-dominated layer that is pushed seaward. The current velocity ranged around 10 cm/s. From mid-depth to the bottom, we clearly see a typical counterclockwise circulation with water flowing seaward on the western part of the calanque and flowing inside the calanque on the eastern part. The 3 transects provide evidence of current acceleration from the end of the calanque (inland) to the mouth of the calanque that opens seaward, and from the surface to the bottom.

At the entrance of the calanque (Transect 1), the depth-averaged current velocity reaches 20 cm/s seaward and 35 cm/s landward. Within the calanque (Transect 2), the water flows are characterized by a weaker current (0-20 cm/s). The 3rd transect obtained above the main spring is characterized by a non homogeneous weak current. Note that the 10 m-layer figure is not displayed here due to the shallow bathymetry. However, the data show that the surface layer is pushed eastward and the depth averaged current still reveals both structures.

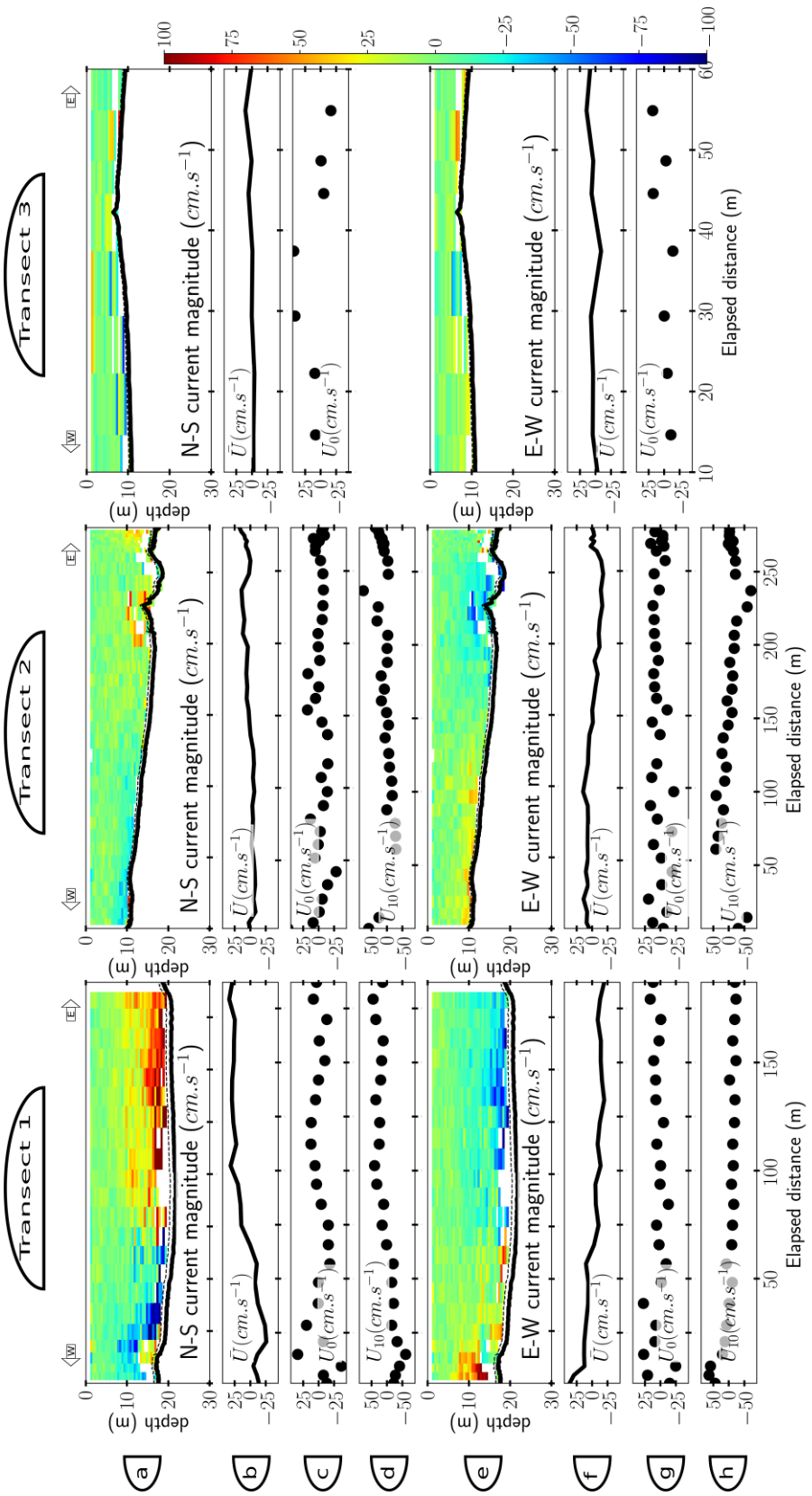

Figure 6: Selected transects (T1: entrance of the calanque, T2, within the calanque, and T3: above the spring) depicting in a): the NS current magnitude profiles, b): the depth-averaged NS current magnitude, c): the near-surface NS current magnitude, d): the near-bottom NS current magnitude, e) the EW current magnitude profile, f): the depth-averaged EW current magnitude, g): the near-surface EW current magnitude, h): the near-bottom EW current magnitude. Positive velocities are oriented

northward on N-S magnitude transects. Positive velocities are oriented eastward on W-E magnitude transects.

6. Discussion

The method generally used to estimate the flux of SGD with a Ra mass balance requires evaluating: 1) other potential non-SGD sources and sinks, 2) the volume of the study site affected by SGD (the "box"), 3) the residence time of coastal waters and 4) the representative concentration of Ra in the discharging groundwater (Charette et al., 2008; Gonneea et al., 2013). In the following, we will first characterize the area in terms of volume, salinity and radium average activities. Then we will discuss a method to estimate the Ra flux offshore as well as the water fluxes exchanged with the sea. Finally we will compare our estimations of SGD to the values measured upstream of the dam in the karst conduit connected to the springs, to discuss the accuracy and the sensitivity of the mass balance approach in this study. The SGD was calculated using the radium isotope mass balance for the two measurement campaigns in July 2012 and September 2014 (Table 3).

6.1 Characterizing the conceptual box and end-members in stratified waters

6.1.1 The volume of the box affected by SGD

The Gulf of Lion is a microtidal environment with a tidal range of 0.30 m at mean spring tides (Aleman et al., 2015). This range associated to the morphology of the calanque does not favor vertical mixing and explains why the water column is stratified (Fig 3). In front of the main spring at 10 m depth the salinity of the water is close to the seawater value (Fig. 3) suggesting that the water coming from the main spring does not mix at the bottom.

This stratification makes it possible to better characterize the shape and volume of the box that needs to be used for the mass balance. The shape is constrained by both sides of the calanque and is closed at the location of PM12 (Fig. 1), where the salinity and radium activities are similar to those of the coastal seawater. This represents a surface area of 125 000 m^2.

The deep layer is saltier, colder and contains a very low amount of radium (Fig. 3). It displays the characteristics of the coastal seawater. The surface layer is less salty, warmer and significantly enriched in radium isotopes as a consequence of the discharge from the submarine karstic springs. Based on profiles measured in 2014, the bottom of this surface layer is located between 1.25 and 2 m deep depending on the location, with an average value of 1.5 m deep. We therefore consider for the mass balance a box displaying a volume of 1.5 x 125 000 i.e. 187 500 m^3.

6.1.2 SGD and seawater end-members

The almost equal salinity and radium activities (Table 1, Fig. 4) measured in the five groundwater samples collected in the karst conduit upstream of the dam or in the spring show that the discharging groundwater is similar in the two sampling points. This suggests that the composition of the karstic water is homogenous and therefore indicates that in this case, the SGD end-member is well identified and its composition well known. Therefore the existence of the dam means that the SGD end-member can be sampled directly, and this adds to the benefit of the radium mass balance model while in many other studies this term is hard to estimate. To calculate the mass balance for July 2012 and September 2014 we used the radium and salinity data measured a few days before each campaign (Table 3).

Below 1.5 m deep in the calanque, the water is not influenced by the groundwater, at least in our vertical profile. Salinity and radium isotopes reach a constant value, consistent with those from the coastal water. The salinity and ^{223}Ra and ^{224}Ra values taken as representative for the seawater in 2012 and 2014

(38 g/L, 0.02 and 0.4 Bq/m^3 respectively) are the values measured at depth below the mixing layer I (Table 3, Fig. 3 and 5).

6.1.3 Average water within the box

Estimating a representative value of the water within the conceptual box is more complicated due to the spatial variations in the calanque surface layer (Table 4, Fig. 1). The arithmetic means for the salinity, ^{224}Ra, ^{223}Ra, ^{228}Th and ^{227}Ac data of the calanque were compared to the means weighted by the percentage of the total surface surrounding each station, calculated using Voronoi polygons. Within uncertainties (1σ standard deviation), no significant differences were found between arithmetic and weighted means for either radium or salinity (Table 3). In the following, the arithmetic means will be considered for all calculations (Table 3).

6.2 Estimating the karstic submarine groundwater discharge: precision and accuracy of the method

The flux of radium from the karstic submarine groundwater discharge, Ra_{SGD} can be estimated using equation (7). The flux of radium exported offshore (Ra_{off}) was calculated according to equations (6) and (9). The apparent age of the calanque surface water (T_w, equation (9)) was 2 ± 1 and 1 ± 0.5 days for the sampling period of 2012 and 2014, meaning on average 1 ± 1 day. These results are similar to the water age estimated using ^{224}Ra and ^{228}Ra isotopes measured in Port-Miou in 2009 (0.7 to 1.6 days; Bejannin et al. 2017). This result is also consistent with our approximation of using the A_{Ra} values measured 1 day before the date of sampling in the calanque of Port-Miou for the mass balance. Using these values of T_w and the radium data (A_{Ra}) reported in Table 3, the calculation of (Ra_{off}), the flux of ^{223}Ra and ^{224}Ra between the calanque and the coastal area, provide similar results for 2012 and 2014 within errors (Table 4). The terms of radium production (Ra_{prod}) and decay (Ra_{dec}) in the box studied were calculated (Table 4) using the volume and the activities of ^{224}Ra, ^{223}Ra ^{228}Th and ^{227}Ac for the calanque (discussed in section 6.1.3).

The different inputs and outputs of the radium mass balance in Table 4 shows that a flux of radium needs to be added to compensate the loss by decay and export. This radium flux (Ra_{SGD}) may be ascribed to groundwater discharge.

The groundwater discharge of the karstic spring of Port-Miou (Q_{SGD}) can therefore be calculated by dividing the flux of radium Ra_{SGD} by the activity of the spring (eq. (8), Table 4).

The values obtained are very low (arithmetic mean of 0.6 ± 0.1 m3/s) but significant within the errors propagated for all terms of the mass balance. The fact that the mass balances calculated for ^{223}Ra and ^{224}Ra isotopes and for two different periods (2012 and 2014) are very similar is an argument that our approach is robust. These values compare fairly well with the estimation made by Bejannin et al. (2017) on the same area but with ^{228}Ra. They obtained a terrestrial groundwater flux of 0.6 to 1.2 m^3/s using data collected in July 2009.

However, these values are significantly lower than the water discharge measured at the dam: 0.6 ± 0.1 versus 4 ± 1 m^3/s. This is surprising because the radium mass balance integrates in the calanque all the inputs from the karstic aquifer, including the small springs from the NE side, as well as possible unknown springs if they have the same radium activities (Fig. 1). Therefore one should expect the Q_{SGD} value estimated with radium isotopes to be higher by at least a factor of 5. Since the discharge measurement of Q_{SGD} at the dam is reliable to within 25%, it appears that our estimation of the Q_{SGD} using the ^{223}Ra-^{224}Ra mass balance is precise but not accurate.

The radium mass balance approach has been commonly used in a large number of hydrological settings (Charette et al., 2001; Kim et al., 2005; Beck et al., 2007; Garcia Solsona et al., 2008b; Moore et al., 2008; Ollivier et al., 2008; Gattacecca et al., 2011; Garcia-Orellana et al., 2014; Baudron et al., 2015;

Montiel et al., 2018). It can be simplified by combining equations (5, 6 and 7) where the determination of Q_{in} and Q_{out} is not required. Another method based on the resolution of the water, salt mass balance and the value of the spring discharge measured upstream the dam can be used to calculate the fluxes of water exchanged between the calanque and the coastal sea (Q_{in} and Q_{out}, see section 4.2, equations 11 to 15). This approach is based on the difference in salinity and ^{224}Ra between the coastal water, the calanque and the spring.

Q_{in}, Q_{out} and Q_{SGD} were simulated using the values reported in Table 3 for 2012 and 2014 in the range of their respective uncertainties. All the solutions were calculated and the results show that the distribution of the solutions is a gaussian. The mean Q_{SGD} is 0 ± 2 m^3/s for both the 2012 and 2014 campaigns (Fig. 7).

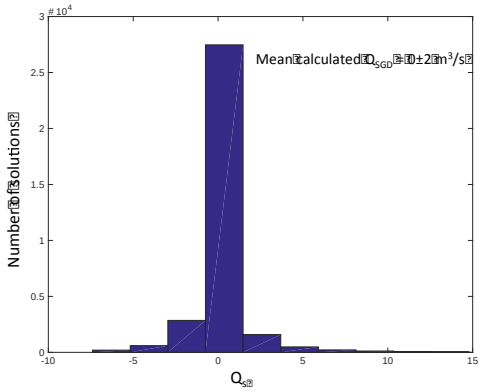

Figure 7: Solutions for Q_{SGD} according to the system of 3 equations based on the data collected in 2014. Q_{SGD} measured during the same period of time is 4±1 m^3/s.

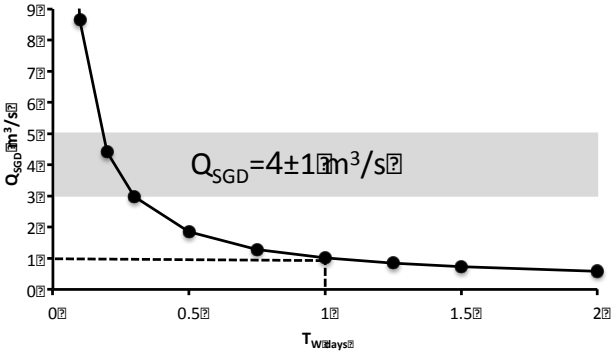

Figure 8: Simulation of Q_{SGD} calculated using ^{224}Ra measurements against the water residence time. The grey bar refers to the Q_{SGD} measured during the sampling period (4±1 m^3/s).

These results are consistent with the previous calculation based on Ra mass balance only. Our results return very similar values when using different data sets (2012, 2014) and both ^{223}Ra and ^{224}Ra. This suggests that at least one parameter in equation (2) plays a key role in the estimation of Q_{SGD}, independently of the radium and salinity measurements in the karstic spring, the calanque of Port-Miou and seawater. We can question the estimation of the volume of the calanque (V). The depth of the layer at which the karstic groundwater mixes has been shown to vary between 1 and 2 m. All the calculations were performed with a value of 1.5m. By propagating an error of ± 0.5 m on the calculation of Q_{SGD}, we obtain a shift in Q_{SGD} value which at most, reaches 0.8 m^3/s. Another key parameter in solving equation (7) is the water residence time (T_W). Our results show that T_W is short relative to the decay period of ^{224}Ra. The very good correlation between ^{224}Ra and salinity (Fig. 5) is another indication that mixing between the karstic springs and the water in the calanque is almost instantaneous. Our estimations of T_W are not very precise (T_W = 1 ± 1 days). Propagating the error on T_W has a strong impact on the calculated Q_{SGD}. Figure 8 shows that the calculated Q_{SGD} value follows an exponential decrease with increasing T_W. T_W is taken to vary over the range 1 ± 1 day. The reference value of Q_{SGD} measured at the dam (4 ± 1 m^3/s) is obtained for a residence time of c.a. 0.2 days, which is about 5 hours while for T_W = 1 day, the Q_{SGD} simulated value is 1 m^3/s. In such cases, where the water residence time is short, the estimation of Q_{SGD} based on radium mass balance cannot be accurate.

Finally, the inaccuracy of the estimation may be associated to a particular hydrodynamic setting in this area. We suggest that the water exchange between the calanque and the open sea is made through an output in the surface layer and an equivalent input in the deeper layer. However, the ADCP profiles

show that there is already an exchange within the deep layer, with strong currents entering the calanque on the east and exiting on the west (Fig. 6). It is thus possible that part of the entire discharge of the groundwater coming from the deep spring is entrained within this deep circulation and exits the calanque without feeding the surface layer. In this case, the SGD occurring in the surface water will be mainly or only due to the surface springs, and this may explain the lower value obtained.

7. Conclusions

In this work we have reported ^{223}Ra, ^{224}Ra, salinity profiles and current measurements in order to understand the degree of precision and accuracy with which we can estimate the submarine groundwater discharge of a main karstic spring, discharging at 10 m depth in a cove (the Port-Miou "calanque"). The cove water is consequently stratified as two different water masses can be distinguished: the shallower water mass (1.5 m deep, on average), brackish and cool, and the deeper water mass which displays the temperature and salinity characteristics of sea water. Water, salinity and radium mass balances were performed in the shallower mixing box to estimate the submarine groundwater discharge (Q_{SGD}). The mean value obtained with ^{223}Ra and ^{224}Ra is precise but significantly lower (0.6 ± 0.1 m^3/s) than direct measurements of the groundwater discharge available inland, in the karst conduit 500 meters upstream the main Port-Miou submarine spring (4 ± 1 m^3/s). The residence time of the cove water estimated using both ^{224}Ra and ^{223}Ra isotopes is very low (1 ± 1 day). First, a high uncertainty for a low water residence time propagates exponentially onto the calculated Q_{SGD}. Second, we suggest that the shape and geometry of the cove, as well as the location of the discharge point of the spring play a key role in explaining these discrepant results. The water circulation in the cove at the location of the karstic spring discharge favors the export of the groundwater in the deeper water mass and decreases the contribution of the karstic spring into the shallower mixing box that was considered for the mass balance calculations. We therefore conclude that in such a stratified Mediterranean cove, the estimations of SGD based on short-lived radium isotopes have to be used with caution if the circulation pattern of the cove water is not well understood.

8. Appendix

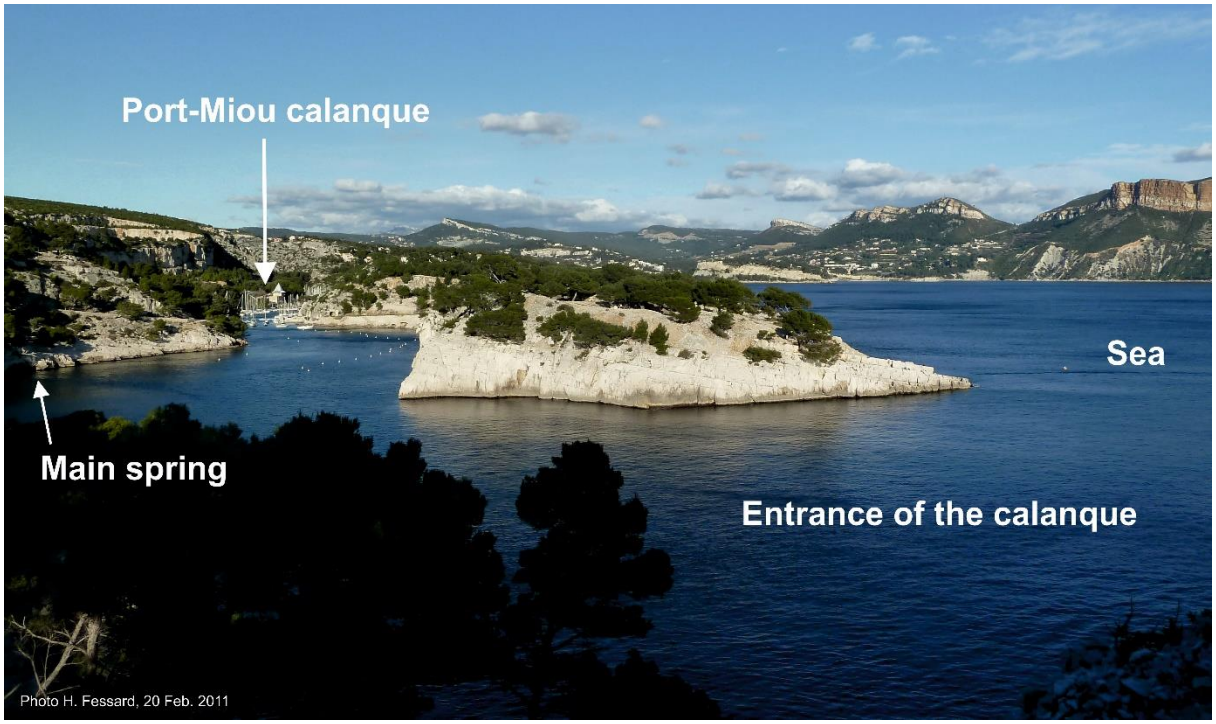

A 1: Panoramic view of the Port-Miou calanque (Cassis, SE France).

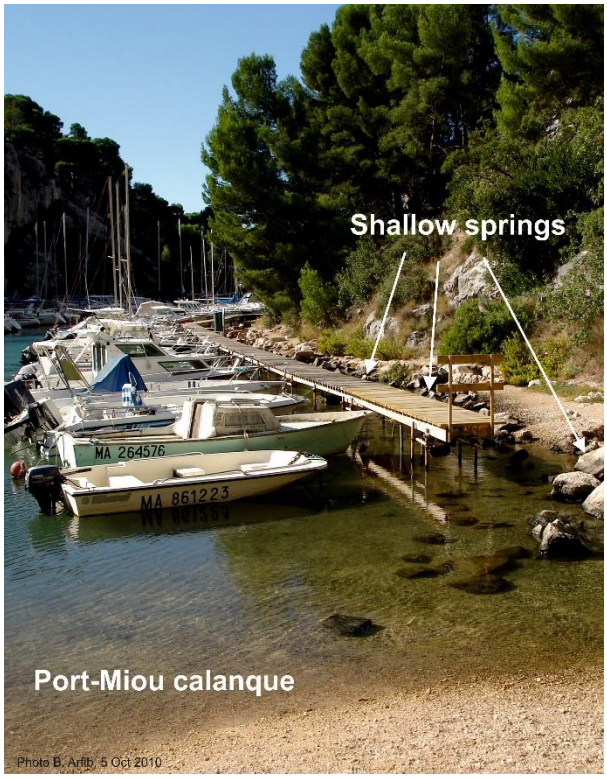

A2: At the northern part of the Port-Miou calanque, brackish springs outflow close to the sea level, in the faulted tight urgonian limestones.

9. References

Aleman N., Robin N., Certain R., Anthony E.J., Barusseau J.P., 2015. Longshore variability of beach states and bar types in a microtidal storm-influence, low-energy environment. Geomorphology 241, 175-191.

Amont and Kerouel, 2004. Hydrologie des écosystèmes marins ; paramètres et analyses » Ed IFREMERenvlit.ifremer.fr/var/envlit/storage/documents/dossiers/prelevementhydro/chapitre8.html.

Arfib, B. and Charlier, J.-B, 2016. Insights into saline intrusion and freshwater resources in coastal karstic aquifers using a lumped rainfall-discharge-salinity model (the Port-Miou brackish spring, SE France). J. Hydrol. 450, 148-161.

Bakalowicz M., 2015. Karst and karst groundwater resources in the Mediterranean. Environmental Earth Sciences, 74, 1, 5–14.

Baudron P., Cockenpot S., López Castejón F., Radakovitch O., Gilabert J., Mayer A., García Aróstegui J.-L., Martinez-Vicente D., Leduc C., Claude C., 2015. Combining Radon, short-lived Radium isotopes and hydrodynamic modeling to assess submarine groundwater discharge from an anthropized semiarid watershed to a Mediterranean lagoon (Mar Menor, SE Spain). J. Hydrol. 525, 55-71.

Beck A.J., Rapaglia J.P., Cochran J.K., Bokuniewicz H.J., 2007. Radium mass-balance in Jamaica Bay, NY: Evidence for a substantial flux of submarine groundwater. *Marine Chemistry* 106, 419–441.

Bejannin, S., van-Beek, P., Stieglitz, T., Souhaut, M. and Tamborski, J., 2017, Combining airborne thermal infrared images and radium isotopes to study submarine groundwater discharge along the French Mediterraean coastline, J. of hydrology: regional studies, 17, 72-90.

Burnett, W.C., Dulaiova, H., 2003. Estimating the dynamics of groundwater input into the coastal zone via continuous radon-222 measurements. J. Environ. Radioact. 69, 21–35. doi:10.1016/S0265-931X(03)00084-5.

Burnett, W.C., Dulaiova, H., 2006. Radon as a tracer of submarine groundwater discharge into a boat basin in Donnalucata, Sicily. Cont. Shelf Res. 26, 862–873. doi:10.1016/j.csr.2005.12.003.

Cerdà-Domènech, M., Rodellas, V., Folch, A., Garcia-Orellana, J. 2017. Constraining the temporal variations of Ra isotopes and Rn in the groundwater end-member: Implications for derived SGD estimates. Science of The Total Environment, Volume 595, Pages 849-857, https://doi.org/10.1016/j.scitotenv.2017.03.005.

Charette M.A., Moore W.S., Burnett W.C., 2008. Uranium- and Thorium-Series Nuclides as Tracers of Submarine Groundwater Discharge (in U-Th Series Nuclides in Aquatic Systems), in: *Radioactivity in the Environment*. Elsevier, 155–191. doi:10.1016/S1569- 4860(07)00005-8.

Charette, M.A., Buesseler, K.O., Andrews, J.E., 2001. Utility of radium isotopes for evaluating the input and transport of groundwater-derived nitrogen to a Cape Cod estuary. Limnol. Oceanogr. 46, 465–470.

Chen, Z., A. Auler, M. Bakalowicz, D. Drew, F. Griger, J. Hartmann, Jiang G., Moosdorf N., RichtsA, Stevanovic Z., Veni G, Goldscheider N., 2017. The world karst aquifer mapping project: Concept, mapping procedure and map of Europe. Hydrogeol. J. 25:771–785. doi:10.1007/s10040-016-1519-3

Cockenpot, S. 2016, Caractérisation des processus aux interfaces air-eau et sédiments-eau pour la quantification des apports d'eaux souterraines par le radium et le radon, PhD, Aix-Marseille University.

Custodio, E., 2010. Coastal aquifers of Europe: an overview. Hydrogeol. J. 18, 269–280.

Ferguson, G., & Gleeson, T. 2012, Vulnerability of coastal aquifers to groundwater use and climate change, Nature Clim. Change, 2, 342-345. DOI: 10.1038/NCLIMATE1413.

Fleury P., Bakalowicz M. and De Marsily G., 2007. Submarine springs and coastal karst aquifers: A review. *Journal of Hydrology*, 339: 79-92.

Ford D., Williams P., 2007. Karst Hydrogeology and Geomorphology. Wiley.

Garcia-Orellana J., Cochran J.K., Bokuniewicz H., Daniel J.W.R., Rodellas V., Heilbrun C., 2014. Evaluation of ^{224}Ra as a tracer for submarine groundwater discharge in Long Island Sound (NY). *Geochimica et Cosmochimica Acta* 141, 314–330. doi:10.1016/j.gca.2014.05.009

Garcia-Solsona E., Garcia-Orellana J., Masqué P., Dulaiova H., 2008b. Uncertainties Associated with ^{223}Ra and ^{224}Ra Measurements in Water via a Delayed Coincidence Counter (RaDeCC). *Marine Chemistry* 109 (3-4): 198–219. doi:10.1016/j.marchem.2007.11.006.

Garcia-Solsona E., Garcia-Orellana J., Masqué P., Garcés E., Radakovitch O., Mayer A., Estradé S., Basterretxea G., 2010a. An assessment of karstic submarine groundwater and associated nutrient discharge to a Mediterranean coastal area (Balearic Islands, Spain) using radium isotopes. *Biogeochemistry* 97, 211–229.

Garcia-Solsona E., Garcia-Orellana J., Masqué P., Rodellas V., Mejías M., Ballesteros B., Domínguez J.A., 2010b. Groundwater and Nutrient Discharge through Karstic Coastal Springs (Castelló, Spain). *Biogeosciences* 7 (9): 2625–38. doi:10.5194/bg-7-2625-2010.

Garcia-Solsona E., Masqué P., Garcia-Orellana J., Rapaglia J., Beck A.J., Cochran J.K., Bokuniewicz H.J., Zaggia L., Collavini F., 2008a. Estimating Submarine Groundwater Discharge around Isola La Cura, Northern Venice Lagoon (Italy), by Using the Radium Quartet. *Marine Chemistry* 109 (3-4): 292–306. doi:10.1016/j.marchem.2008.02.007.

Gattacceca J.C., Mayer A., Cucco A., Claude C., Radakovitch O., Vallet-Coulomb C., Hamelin B., 2011. Submarine groundwater discharge in a subsiding coastal lowland: A ^{226}Ra and ^{222}Rn investigation in the Southern Venice lagoon. *Applied Geochemistry* 26, 907–920.

Gonneea, M.E., Mulligan, A.E., Charette, M.A., 2013. Seasonal cycles in radium and barium within a subterranean estuary: Implications for groundwater derived chemical fluxes to surface waters. Geochim. Cosmochim. Acta 119, 164–177. doi:10.1016/j.gca.2013.05.034

Johannes, R., 1980, Ecological significance of the subterranean discharge of groundwater, mar. Ecol. Prog. Ser., 365-73.

Kim G., Lee K.-K., Park K.S., Hwang D.W., Yang H.S., 2003. Large submarine groundwater discharge (SGD) from a volcanic island. *Geophysical Research Letters* 30 (21).

Kim, G., Kim, S.-J., Harada, K., Schultz, M.K., Burnett, W.C., 2005. Enrichment of Excess 210Po in Anoxic Ponds. Environ. Sci. Technol. 39, 4894–4899. doi:10.1021/es0482334

Knee, K.L., Paytan, A., 2011. Submarine Groundwater Discharge: A Source of Nutrients, Metals, and Pollutants to the Coastal Ocean, in: Wolanski, E., McLusky, D. (Eds.), *Treatise on Estuarine and Coastal Science*. Elsevier, pp. 205–233. doi:10.1016/B978-0-12-374711-2.00410-1

Lamontagne, S., Taylor, A.R. Herpich, D., Hancock, G.J., 2015. Submarine groundwater discharge from the South Australian Limestone Coast region estimated using radium and salinity. Journal of Environmental Radioactivity, Volume 140, Pages 30-41, https://doi.org/10.1016/j.jenvrad.2014.10.013.

Ludwig, W., Dumont, E., Meybeck, M., Heussner, S., 2009. River discharges of water and nutrients to the Mediterranean and Black Sea: Major drivers for ecosystem changes during past and future decades? Prog. Oceanogr. 80, 199–217. doi:10.1016/j.pocean.2009.02.001

Monsen, N.E., Cloern, J.E., Lucas, L. V., Monismith, S.G., 2002. A comment on the use of flushing time, residence time, and age as transport time scales. Limnol. Oceanogr. 47, 1545–1553.

Montiel D., Dimova, N., Andreo, B., Prieto, J., García-Orellana, J., Rodellas, V. 2018 Assessing submarine groundwater discharge (SGD) and nitrate fluxes in highly heterogeneous coastal karst

aquifers: Challenges and solutions, Journal of Hydrology, Volume 557, Pages 222-242, https://doi.org/10.1016/j.jhydrol.2017.12.036.

Moore W.S., 1996a. Large Groundwater Inputs to Coastal Waters Revealed by ^{226}Ra Enrichments. *Nature* 380 (612-614).

Moore W.S., 1996b. Using the radium quartet for evaluating groundwater input and water exchange in salt marshes, Geoch. Cosmoch. Acta, 60, 4645-4652.

Moore W.S., 2008. Fifteen years experience in measuring ^{224}Ra and ^{223}Ra by delayed-coincidence counting. *Marine Chemistry* 109, 188–197.

Moore, W.S., 2000. Ages of continental shelf waters determined from ^{223}Ra and ^{224}Ra. J. Geophys. Res. C Ocean. 105, 22117–22122.

Moore, W.S., 2003. Sources and fluxes of submarine groundwater discharge delineated by radium isotopes. Biogeochemistry 66, 75–93. doi:10.1023/B:BIOG.0000006065.77764.

Moore, W.S., 2010. The Effect of Submarine Groundwater Discharge on the Ocean. Ann. Rev. Mar. Sci. 2, 59–88. doi:10.1146/annurev-marine-120308-08101

Moore, W.S., Blanton, J.O., Joye, S.B., 2006. Estimates of flushing times, submarine groundwater discharge, and nutrient fluxes to Okatee Estuary, South Carolina. J. Geophys. Res. 111, C09006. doi:10.1029/2005JC003041

Moore, W.S., Sarmiento, J.L., Key, R.M., 2008. Submarine groundwater discharge revealed by 228Ra distribution in the upper Atlantic Ocean. Nat. Geosci. 1, 309–311. doi:10.1038/ngeo183

Moosdorf, N., & Oehler, T. 2017. Societal use of fresh submarine groundwater discharge: An overlooked water resource. Earth-Science Reviews, 171, 338–348. https://doi.org/10.1016/j.earscirev.2017.06.006

Ollivier, P., Claude, C., Radakovitch, O., Hamelin, B., 2008. TIMS measurements of ^{226}Ra and ^{228}Ra in the Gulf of Lion, an attempt to quantify submarine groundwater discharge. Mar. Chem. 109, 337–354. doi:10.1016/j.marchem.2007.08.006

Peterson, R.N., Burnett, W.C., Glenn, C.R., Johnson, A.G., 2009. Quantification of point-source groundwater discharges to the ocean from the shoreline of the Big Island, Hawaii. Limnol. Oceanogr. 54, 890–904.

Rapaglia J., Ferrarin C., Zaggia L., Moore W.S., Umgiesser G., Garcia-Solsona E., Garcia-Orellana J., Masque P., 2010. Investigation of residence time and groundwater flux in Venice Lagoon: comparing radium isotope and hydrodynamical models. *Journal of Environmental Radioactivity* 101, 571–581.

Rodellas V., Garcia-Orellana J., Masqué P., Feldman M., Weinstein Y., 2015. Submarine Groundwater Discharge as a Major Source of Nutrients to the Mediterranean Sea. *Proceedings of the National Academy of Sciences* 112 (13): 3926–30. doi:10.1073/pnas.1419049112.

Santos, I.R., Eyre, B.D., Huettel, M., 2012. The driving forces of porewater and groundwater flow in permeable coastal sediments: A review. Estuar. Coast. Shelf Sci. 98, 1–15. doi:10.1016/j.ecss.2011.10.024

Schnegg P.A., Perret, C., Hauet, A., Parrel, D., Saysset, G., Vignon, P., 2011. Stream gauging by dilution of fluorescent tracers and state of the art of the EDF hydroclimatological observation network. 9th conference on limestone hydrogeology, Besançon, France

Scholten, J.C., Pham, M.K., Blinova, O., Charette, M.A., Dulaiova, H., Eriksson, M., 2010. Preparation of Mnfiber standards for the efficiency calibration of the delayed coincidence counting system (RaDeCC). Mar. Chem. 121, 206–214. doi:10.1016/j.marchem.2010.04.009

Slomp C.P. and Van Cappellen P., 2004. Nutrient inputs to the coastal ocean through submarine groundwater discharge: controls and potential impact. *Journal of Hydrology* 295, 64–86. doi:10.1016/j.jhydrol.2004.02.018

Stieglitz, T.C., van-Beek, P., Souhaut, M., Cook, P.G., 2013. Karstic groundwater discharge and

seawater recirculation through sediments in shallow coastal Mediterranean lagoons, determined from water, salt and radon budgets. Mar. Chem. 156, 73–84. doi:10.1016/j.marchem.2013.05.005

Sun, Y., Torgersen, T., 1998. The effects of water content and Mn-fiber surface conditions on measurement by emanation. Mar. Chem. 62, 299–306. doi:10.1016/S0304-4203(98)00019-X

Swarzenski, P.W., 2007. U/Th series radionuclides as coastal groundwater tracers. Chem. Rev. 107, 663–74.doi:10.1021/cr0503761

Tulipano L., Fidelibus M. D., Panagopoulos A., 2005. Groundwater management of coastal karstic aquifers. COST 621 report, EUR21366EN. 363p

UNESCO: Submarine groundwater discharge, Management implications, measurements and effects, Paris, United Nations Educational, Scientific and Cultural Organization IHP-VI, Series on Groundwater, 5, 2004.

Waska, H. & Kim, G., 2011. Submarine groundwater discharge (SGD) as a main nutrient source for benthic and water-column primary production in a large intertidal environment of the Yellow Sea. Journal of Sea Research, 65(1), 103–113. doi:10.1016/j.seares.2010.08.001.

10. Acknowledgments

The project was funded by i) the WP3/MERMEX/MISTRALS program and is a contribution to the international LOICZ program, ii) ANR-MED-SGD (ANR-15-CE01-0004), iii) Région PACA for the funding of the project "SOURCES" through the APEX2013_04244. The authors would like to thank the KARST observatory network (SNO KARST) initiative at the INSU/CNRS, which aims to strengthen knowledge-sharing and promote cross-disciplinary research on karst systems at the national scale. We also thank ''Météo France" for the meteorological data, the ''Conservatoire du Littoral" for access to the Port-Miou in-situ underground laboratory and two anonymous reviewers for their helpful comments.
www.sokarst.org
www.karsteau.fr

TABLE

Sample type	Sampling date	Salinity	T°C	^{224}Ra (Bq/m^3)	^{223}Ra (Bq/m^3)
Spring	23/07/12	11.9	17.2	22±1	2.6±0.3
Dam	08/01/13	9.7	16.0	22±1	2.5±0.3
Spring	08/01/13	9.7	16.0	22±1	1.6±0.2
Dam	06/03/13	10.0	16.9	22±2	2.0±0.3
Dam	29/08/14	10.1	17.4	25±1	2.3±0.2
Arithmetic mean		10.2±0.8		23±1	2.2±0.4

Table1: Salinity, temperature and ^{224}Ra, ^{223}Ra activities measured in spring and dam groundwater samples. Uncertainties are 1σ.

Sample name	Type of water	Sampling date (dd/mm/yy)	Sample depth m	Total depth m	Salinity	T (°C)	^{224}Ra (Bq/m^3)	^{223}Ra (Bq/m^3)	^{228}Th (Bq/m^3)	^{227}Ac (Bq/m^3)
PM1	CW	25/07/12	0	79	38.5	19.3	0.20±0.01	0.008±0.003	nd	nd
PM2	CW	25/07/12	0	56.4	37.1	18.3	0.41±0.02	0.04±0.01	nd	nd
PM3	CW	25/07/12	0	60.5	37.3	19.5	0.25±0.02	0.015±0.004	nd	nd
PM4	CW	25/07/12	0	35.6	37.0	18.6	0.40±0.04	0.04±0.01	nd	nd
PM5	CW	25/07/12	0	38	36.9	18.8	0.50±0.04	0.04±0.01	nd	nd
PM6	CW	25/07/12	0	48.2	36.7	18.5	0.70±0.03	0.06±0.01	nd	nd
PM7_Surf	CW	25/07/12	0	26	34.5	18.4	2.00±0.10	0.21±0.03	nd	0.02±0.01
PM7_Mid	CW	25/07/12	12	26	37.3	nd	0.50±0.04	0.02±0.01	nd	nd
PM7_deep	CW	25/07/12	24	26	37.1	nd	0.40±0.02	0.02±0.01	nd	nd
PM8	CAL	26/07/12	0	20	29.7	19.5	7.4±0.6	0.8±0.1	nd	0.03±0.02
PM9	CAL	26/07/12	0	18	30.3	19.7	6.3±0.4	0.9±0.1	nd	0.10±0.04
PM10	CAL	26/07/12	0	10	24.4	19.0	12±1	1.0±0.2	nd	0.10±0.03
PM Cap_surf	CAL	08/01/13	0	4.5	22.0	nd	13±1	1.0±0.2	nd	nd
PM Cap_1m	CAL	08/01/13	1	4.5	31.5	nd	4.7±0.4	0.7±0.1	nd	nd
PM Cap_surf	CAL	29/08/14	0	4.5	23.7	22	12.0±0.7	1.6±0.1	0.8±0.1	nd
PM Cap_0.75	CAL	29/08/14	0.75	4.5	31.3	21.5	5.7±0.2	0.7 ±0.1	0.40±0.05	nd
PM Cap_1m25	CAL	29/08/14	1.25	4.5	35.0	21.2	2.3±0.1	0.20±0.04	0.20±0.03	nd
PM Cap_2.50	CAL	29/08/14	2.50	4.5	35.1	21	2.9±0.2	0.20±0.04	0.20±0.03	nd
PM11	CW	01/09/14	0	38	35.0	18.7	2.5±0.1	0.20±0.02	0.20±0.02	nd
PM12	CW	01/09/14	0	25	36.7	18.0	1.2±0.1	0.10±0.02	0.20±0.02	nd
PM13	CAL	01/09/14	0	22	32.9	18.2	4.3±0.2	0.40±0.04	0.30±0.02	nd
PM14	CAL	01/09/14	0	16	27.2	18.6	8.1±0.5	1.0±0.1	0.6±0.1	nd
PM15	CAL	01/09/14	0	12	28.3	19.4	8.6±0.3	0.9±0.1	0.6±0.1	nd
PM16	CAL	01/09/14	0	10	29.9	18.9	6.2±0.2	0.6±0.1	0.50±0.04	nd
PM17	CAL	01/09/14	0	10	25.8	19.6	9.5±0.4	1.0±0.1	0.70±0.1	0.10±0.01
PM18	CAL	01/09/14	0	8.5	27.1	19.0	8.6±0.5	1.1±0.1	0.6±0.1	nd
PM19	CAL	01/09/14	0	5.5	29.1	21.0	7.4±0.4	0.8±0.1	0.6±0.1	nd
PM20	CAL	01/09/14	0	5	24.6	20.6	11.5±0.6	1.3±0.2	0.7±0.1	nd
PM21	CAL	01/09/14	0	4	34.4	20.9	4.8±03	0.5±0.1	0.30±0.03	nd
PM22	CAL	01/09/14	0	5	35.5	21.2	4.6±0.2	0.4±0.1	0.20±0.02	nd
PM23	CAL	01/09/14	0	6.5	35.1	21.3	4.9±0.3	0.5±0.1	0.40±0.04	nd
PM24	CAL	01/09/14	0	5.5	34.6	21.5	5.9±0.3	0.5±0.1	0.20±0.02	nd
PM25	CAL	01/09/14	0	4	34.1	21.5	5.9±0.4	0.6±0.1	0.30±0.04	nd
PM26	CAL	01/09/14	0	3	27.4	21.4	12.0±0.8	1.2±0.2	0.8±0.1	nd

Table 2: Salinity, temperature and ^{224}Ra, ^{223}Ra, ^{228}Th and ^{227}Ac activities measured in the calanque of Port-Miou (CAL) and in coastal seawater (CW). The sample depth and the total depth of the water column are also indicated. Uncertainties are 1σ.

	Salinity	^{224}Ra (Bq/m^3)	^{223}Ra (Bq/m^3)	^{228}Th (Bq/m^3)	^{227}Ac (Bq/m^3)
2012					
Spring	11.9±0.2	22±1	2.6±0.3		
Calanque (Arith. mean)	28±2	9±3	0.9±01	nd	0.06±0.01
Sea water	38.0±0.3	0.4±0.1	0.03±0.02		
2014					
Spring	10.1±0.2	25±1	2.3±0.2	1.7±0.1	
Calanque (Arith. mean)	30±4	7±3	0.8±0.3	0.5±0.1	0.11±0.01
Sea water	38.0±0.3	0.4±0.1	0.03±0.02	0.2±0.02	

Table 3: Salinity and ^{224}Ra, ^{223}Ra, ^{228Th} and ^{227}Ac activities taken as representative values for the spring groundwater endmember, sea water and the calanque of Port-Miou used for the mass balance calculation. Uncertainties are 1σ.

MASS BALANCE	2012 ^{224}Ra	2012 ^{223}Ra	2014 ^{224}Ra	2014 ^{223}Ra	Units
Inputs					
Ra_{prod} : production from parent in water (λ*activity$_P$*V) eq. (3)	nd	0.7±0.2 10^2	1.8±0.3 10^4	1.3±0.1 10^3	Bq/d
TOTAL INPUTS	**nd**	**0.7±0.2 10^3**	**1.8±0.3 10^4**	**1.3±0.1 10^3**	**Bq/d**
Outputs					
Ra_{decay} : decay of tracers in the studied volume (activity$_{PM}$*V$_{PM}$*λ) eq. (4)	30±10 10^4	10±1 10^3	25±11 10^4	9±3 10^3	Bq/d
Ra_{off}: output flux budget to the Mediterranean Sea (Ra_{out} – Ra_{in}) eq. (5)	70±40 10^4	70±30 10^3	110±60 10^4	130±80 10^3	Bq/d
TOTAL OUTPUTS	**100±40 10^4**	**80±30 10^3**	**140±60 10^4**	**140±80 10^3**	**Bq/d**
Ra_{SGD}: Submarine Groundwater Discharge flux of tracers, estimated by difference between output terms and input terms					
activity$_{GW}$: tracer activity in groundwater spring	22	2.6	25	2.3	Bq/m^3
Q_{SGD} Spring flux: F_{SGD} / activity$_{GW}$ eq. (8)	**0.5±0.2**	**0.4±0.2**	**0.6±0.3**	**0.7±0.4**	**m^3/s**

Table 4: Summary of the mass balance calculation for the calanque of Port-Miou. Uncertainties on all radionuclides fluxes are 1σ. The volume of the calanque of Port-Miou mixing with the spring is a box of 1.5m * 125 000m^2 equals 187500 m^3. For the mass calculation of ^{224}Ra in 2012, the production flux was neglected.